Mon. Not. R. Astron. Soc. **000**, 1–?? (2002) Printed 6 October 2008 (MN LATEX style file v2.2)

Morphology Classification and Photometric Redshift Measurement of Galaxies

Yanxia Zhang[1⋆] ,Lili Li[1,2] and Yongheng Zhao[1]
[1] *National Astronomical Observatories, Chinese Academy of Sciences, 20A Datun Road, Chaoyang District, 100012, Beijing, P.R.China*
[2] *Weishanlu Middle School, 300222, Tianjin, P.R.China*

arXiv:0810.0867v1 [astro-ph] 6 Oct 2008

Released 2002 Xxxxx XX

ABSTRACT

Based on the Sloan Digital Sky Survey Data Release 5 Galaxy Sample, we explore photometric morphology classification and redshift estimation of galaxies using photometric data and known spectroscopic redshifts. An unsupervised method, k-means algorithm, is used to separate the whole galaxy sample into early- and late-type galaxies. Then we investigate the photometric redshift measurement with different input patterns by means of artificial neural networks (ANNs) for the total sample and the two subsamples. The experimental result indicates that ANNs show better performance when the more parameters are applied in the training set, and the mixed accuracy $\sigma_{\rm mix} = \sqrt{{\sigma_{\rm early}}^2 + {\sigma_{\rm late}}^2}$ of photometric redshift estimation for the two subsets is superior to $\sigma_{\rm z}$ for the overall sample alone. For the optimal result, the rms deviation of photometric redshifts for the mixed sample amounts to 0.0192, that for the overall sample is 0.0196, meanwhile, that for early- and late-type galaxies adds up to 0.0164 and 0.0217, respectively.

Key words: catalogs - galaxies: distances and redshifts - galaxies: general - galaxies: photometry - surveys - techniques: photometric

1 INTRODUCTION

The Sloan Digital Sky Survey (SDSS, York et al. 2000) is an astronomical survey project, which covers more than a quarter of the sky, to construct the first comprehensive digital map of the universe in 3D. The large amount of spectroscopic and photometric data obtained during the last years by SDSS, which has opened a new horizon for the study of galaxy properties such as galaxy evolution, clusters, redshifts, large-scale distribution on morphological type and so on. However, photometric classification and redshift estimation is of prime importance for the SDSS project. Obtaining reliable object type and redshift estimation based on SDSS photometry is thus an extremely valuable adjunct to the spectroscopic sample.

One of the first segregation discovered in galaxy clusters was the morphological one. The first evidences of such segregation date from Curtis (1918) and Hubble & Humason (1931), and was quantified by Oemler (1974) and Melnick & Sargent (1977). The problem of general automated classification always lies in the difficulty of finding quantitative measures that strongly correlate with the Hubble sequence based on visual inspections. Shimasaku et al. (2001) and Strateva et al. (2001) using SDSS data, showed that the ratio of Petrosian 50 percent light radius to Petrosian 90 percent light radius, C_{in}, measured in the r-band image was a useful index for quantifying galaxy morphology. For early-type galaxies, concentration index C_{in} is larger than 2.5; while for late-type galaxies, C_{in} is less than 2.5. Strateva et al. (2001) also found that the color $u - r = -2.22$ efficiently separates early- and late-type galaxies at $z < 0.4$. The basis for the classification of the SDSS photometric database can be provided by the objects whose nature is precisely known from spectroscopy.

Photometric redshifts refer to the redshift estimation of galaxies using only medium- or broad-band photometry or imaging instead of spectroscopy. Techniques for deriving redshifts from broadband photometry were pioneered by Baum (1962). Subsequent implementations of these basic techniques have been made by Couch et al. (1983) and Koo (1985). In terms of data mining, the photometric redshift estimation belongs to the regression task of data mining. In principal, the various approaches used for solving regression problem may be applied to the photometric redshift measurement. So far there has been a great amount of research on the techniques of photometric redshift estimation. The techniques are broadly grouped into three kinds: the template-matching method, the empirical training-set

⋆ Email: zyx@lamost.org, yzhao@lamost.org

method, instance-based learning method. When using the template-matching method, we must have the template. The quality of template directly influences the performance of predicting photometric redshifts. The template spectra come from population synthesis models (e.g. Bruzual & Charlot 1993) or from spectra of real objects (e.g. Coleman et al. 1980). The empirical training-set method is based on the real data. So whether the real data is enough and complete is an important factor. The training-set method is usually implemented by train-test method or cross-validation method, in other words, it needs to train training-set to get a classifier or regressor and then the classifier or regressor is tested by test set. Typical empirical training-set methods include artificial neural networks (ANNs, Collister & Lahav 2004; Firth, Lahav & Somerville 2003; Vanzella et al. 2004; Li et al. 2007), support vector machines (SVMs, Wadadekar 2005; Wang et al. 2007, 2008), ensemble learning and Gaussian process regression (Way & Srivastava 2006), and linear and non-linear polynomial fitting (Brunner et al. 1997; Wang, Bahcall & Turner 1998; Budavári et al. 2005; Hsieh et al. 2005; Connolly et al. 1995). Although the instance-based learning method also relies on the real data, it is different from the training-set method for it has no training process and stores all data in the memory of computer. Examples of such techniques are k-nearest neighbours (e.g. Csabai et al. 2003; Ball et al. 2007; Gao, Zhang & Zhao 2007), kernel regression (Wang et al. 2007, 2008), and locally weighted regression.

This paper majors in morphological classification of galaxies using k-means algorithm and photometric redshift estimation of galaxies using artificial neural networks (ANNs). The paper is organized as follows. Section 2 gives the scheme of this paper. Section 3 introduces a brief overview of k-means algorithm and artificial neural networks, respectively. Section 4 describes photometric classification of galaxies using k-means algorithm. We investigate redshift estimation using an extensive series of tests in Section 5. The conclusions and discussions are summarized in Section 6.

2 THE SCHEME OF THIS PAPER

This paper demonstrates the potential of bulk classification of the SDSS data and indicates a wide range of research applications, especially for redshift estimation. K-means algorithm offers an efficient way to identify the physical nature of SDSS sources, so it has a strong potential to become an important classification tool for the bulk of the SDSS photometric database. We collect the SDSS Data Release 5 galaxy sample. Then k-means algorithm is applied on this sample for two respects: one is to preprocess the sample by removing outliers; another is to automatically separate preprocessed sample into two morphological classes (namely early- and late-type galaxies). After that, we consider two cases for photometric redshift estimation with different input patterns by artificial neural networks (ANNs). The first is directly to use ANNs on the total preprocessed sample, and the other is to employ ANNs on the early- and late-type galaxies respectively. Finally the results of the two cases are compared.

3 PRINCIPLE

3.1 K-means Algorithm

The k-means algorithm (MacQueen, 1967) is one of the simplest unsupervised learning algorithms used for clustering problem. The algorithm clusters n objects based on attributes into k partitions, $k < n$. The main idea is to define k centroids, one for each cluster. These centroids should be placed in a cunning way because different locations cause different results. So, the better choice is to place them as much as possible far away from each other. The next step is to take each point belonging to a given data set and associate it to the nearest centroid. When no point is pending, the first step is completed and an early groupage is done. At this point we need to re-calculate k new centroids as barycenters of the clusters resulting from the previous step. After we have these k new centroids, a new binding has to be done between the same data set points and the nearest new centroid. A loop has been generated. As a result of this loop we may notice that the k centroids change their location step by step until no more changes are done. In other words centroids do not move any more.

K-means algorithm is similar to the expectation-maximization algorithm for mixtures of Gaussians in that they both attempt to find the centers of natural clusters in the data. It assumes that the object attributes form a vector space. The objective it tries to achieve is to minimize total intra-cluster variance, or, the squared error function

$$V = \sum_{i=1}^{k} \sum_{x_j \in S_i} (x_j - \mu_i)^2 \quad (1)$$

where there are k clusters S_i, $i = 1, 2, 3, ..., k$, and μ_i is the centroid or mean point of all the points $x_j \in S_i$.

Although it can be proved that the procedure will always terminate, the k-means algorithm does not necessarily find the most optimal configuration, corresponding to the global objective function minimum. The algorithm is also significantly sensitive to the initial randomly selected cluster centers. The k-means algorithm can be run multiple times to reduce this effect.

3.2 Artificial Neural Networks

An Artificial Neural Network (ANN) is an information processing paradigm that is inspired by the way biological nervous systems, such as the brain, process information. The key element of this paradigm is the novel structure of the information processing system. ANNs are collections of interconnected neurons each capable of carrying out simple processing. Thus, they are composed of massively parallel distributed processors that have an inherent property of storing experiential knowledge and making it available for use. The knowledge is acquired by the network through a learning process and is stored in interneuron connection strengths - known as synaptic weights (Haykin 1994). Practical applications of ANNs most often employ supervised learning. For supervised learning, one must provide training data that includes both the input (a set of vectors of parameters, here each vector corresponds to a galaxy) and the desired result or the target value (the corresponding redshifts). After the network is trained successfully, one can present input data

alone to the ANN (that is, input data without the desired result), and the ANN will compute an output value that approximates the desired result. This is achieved by using a training algorithm to minimize the cost function which represents the difference (error) between the actual and desired output. The cost function E is commonly of the form

$$E = \frac{1}{p}\sum_{k=1}^{p}(o_k - t_k)^2, \tag{2}$$

where o_k and t_k are the output and target respectively for the objects, p is the sample size. Generally the topology of an ANN can be schematized as a set of N layers (see Fig. 1), with each layer composed of a number of neurons. The first layer ($i = 1$) is usually called the "input layer", the intermediate ones the "hidden layers", and the last one ($i = N$) the "output layer". Such a species of ANN is formally known as a "multilayer perceptron" (MLP). Each neuron j in the s layer derives a weighted sum of the M output z_i^{s-1} from the previous layer $(s-1)$ and, through either a linear or a non-linear function, produces an output,

$$z_i^{(s)} = f(\sum_{i=0}^{M} w_{ji}^{(s)} z_i^{(s-1)}). \tag{3}$$

Here w_{j0} denotes the bias for the hidden unit j, and f is an activation function such as the continuous sigmoid or, as used here, the tanh function, which has an output range of -1 to 1:

$$f(x) = \frac{2}{1 + e^{-2x}} - 1. \tag{4}$$

When the entire network has been executed, the output of the last layer is taken as the output of the entire network. The free parameters of ANNs are the weight vectors. During the training session, the weights of the connections are adjusted so as to minimize the total error function. The learning procedure is the so-called "back propagation". The number of layers, the number of neurons in each layer, and the functions are chosen from the beginning and specify the so called "architecture" of the ANN. Neural networks learn by examples. The neural network user gathers representative data into a training set and initiates the weight vector with a random seed, then invokes the training algorithms to automatically learn the structure of the data. Here, we use a method that is popular in neural network research: the Levenberg-Marquardt method (Levenberg 1944; Marquardt 1963; also detailed in Bishop 1995). This has the advantage that it converges very quickly to a minimum of the error function. This error function may not have just a global minimum in the multidimensional weight space but could have a number of local minima instead. In general, network trained using exactly the same training set for the same given number of epochs but using different initial weights (different starting points in this space) will converge to slightly different final weights. In order to avoid (possible) over-fitting during the training, another part of the data can be reserved as a validation set (independent both of the training and test sets, so not used in the updating of the weights), and used during the training to monitor the generalization error. After a chosen number of training iterations, the training terminates and the final weights chosen for the ANN are those from the iteration at which the cost function is minimal on the validation set. This is useful to avoid over-fitting to the training set when the training set is small, but the disadvantage of this technique is that it reduces the amount of data available for both training and validation, which is particularly undesirable if the data set is small to begin with.

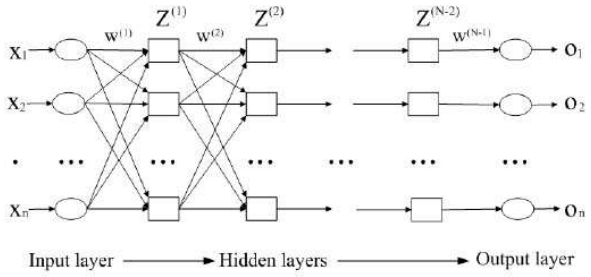

Figure 1. Schematic diagram of an ANN

An ANN is configured for a specific application, such as pattern recognition or data classification, through a learning process. ANNs have various popular applications in astronomy, for example, star/galaxy separation (e.g. Odewahn & Nielsen 1994; Bertin & Arnouts 1996), morphological classification of galaxies (Nielsen & Odewahn 1994; Lahav et al. 1996; Ball et al. 2004), spectral classification (Folkes et al. 1996; Weaver 2000) and astronomical objects classification (Zhang & Zhao 2004, 2007), photometric redshift estimation (e.g., Firth et al. 2003; Vanzella et al. 2004; Li et al. 2007; D'Abrusco et al. 2007). As for a review of ANNs applied in astronomy, refer to Serra-Ricart et al. (1993), Miller (1993), Storrie-Lombardi & Lahav (1994) and Li et al. (2006). Bailer-Jones (1996, 2000) also majored in this issue.

4 MORPHOLOGY CLASSIFICATION

4.1 Chosen Galaxy Sample

The Sloan Digital Sky Survey (SDSS) is the most ambitious astronomical survey ever undertaken. The SDSS uses a dedicated, 2.5-meter telescope on Apache Point, New Mexico, equipped with two powerful special-purpose instruments. The SDSS completed its first phase of operations – SDSS-I – in June, 2005. Over the course of five years, SDSS-I imaged more than 8,000 square degrees of the sky in five bandpasses, detecting nearly 200 million celestial objects, and it measured spectra of more than 675,000 galaxies, 90,000 quasars, and 185,000 stars. These data have supported studies ranging from asteroids and nearby stars to the large scale structure of the Universe. The SDSS has entered a new phase, SDSS-II, continuing through June, 2008. SDSS-II will carry out three distinct surveys - the Sloan Legacy Survey, SEGUE, and the Sloan Supernova Survey - to address fundamental questions about the nature of the Universe, the origin of galaxies and quasars, and the formation and evolution of our own Galaxy, the Milky Way.

We downloaded 582,512 galaxies from the SDSS DR5 database, only took objects with available five-band photometries. By removing the records with default values, we obtained 582,257 galaxies.

4.2 K-means Algorithm for Morphology Classification

The origin of the morphology of galaxies is a longstanding issue that could provide a key to discerning among models of the formation of galaxies. Perhaps there is a general correlation between galaxy color and Hubble morphologies, Strateva et al. (2001) had demonstrated that the galaxy color $u-r$ is related with the morphology of galaxies and grouped galaxies into two families. In this section we also used the galaxy color index to classify the galaxies with k-means algorithm.

As we known, k-means algorithm is an unsupervised approach, and it can automatically cluster based on the intrinsic property of objects. Here we use this approach to cluster the above given sample into two galaxy types (namely early-type and late-type galaxies). For this experiment, we used the five Petrosian color index (u-g, g-r, r-i, i-z, u-r) as the input parameters of k-means approach. The algorithm programme may analyze the color property of the whole sample and separate the given database into two classes automatically. As a result, the number of each family is 300,903 and 281,354, respectively.

In order to verify the type of each class, we randomly select 1000 records from each family respectively to confirm their types, which is achieved by using their position corresponding to the given one in the NASA/IPAC Extragalactic Database (NED). By consulting, we found that the cluster membership with 300,903 records are early-type galaxies and the other 281,354 records belong to late-type galaxies. In Fig. 2 and Fig. 3, we give the $u-r$ histogram for individual subclass (early- and late-type galaxies), respectively. The $u-r$ histogram of the total galaxy sample is shown in Fig. 4. The $g-r$ versus $u-r$ diagram is displayed in Fig. 5, where the samples with red points are early-type galaxies and the ones with black points are late-type galaxies. In Fig. 5, the line is the $u-r=2.22$ plane. According to the $u-r$ cut (Strateva et al. 2001), the galaxies with $u-r>2.22$ belong to early-type galaxies, while those with $u-r<2.22$ belong to late-type galaxies. However, by means of k-means method for classification, the $u-r$ value for early-type galaxies lies in the range from 2.0 to 8.0, that for late-type ones in the range from 0 to 5.0. Therefore the classification results by the two methods show difference. Only by the $u-r$ cut for morphological separation could there be degeneracies. For example, some low redshift dusty edge-on spirals could easily be misclassified as early-type galaxies. As a result, the classification result of k-means method is more reasonable than the $u-r$ cut because this algorithm applies more information and classify objects in a multi-parameter space. K-means algorithm has obvious strength that it is automatically clustering by the properties of galaxies in the real universe and require no additional assumptions about their formation and evolution.

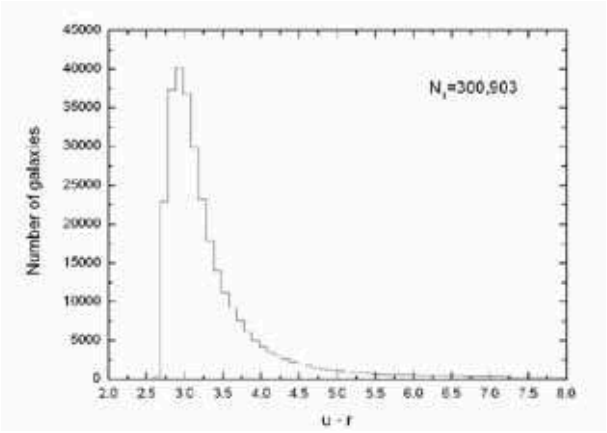

Figure 2. The $u-r$ histogram for early-type galaxies.

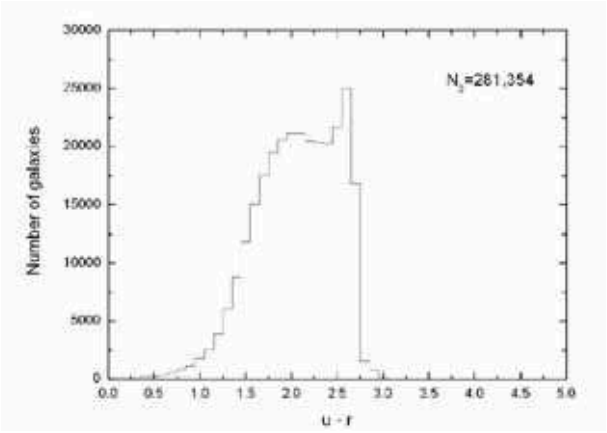

Figure 3. The $u-r$ histogram for late-type galaxies.

5 REDSHIFT ESTIMATION

5.1 The Used Sample

Before the experiment of photometric redshift prediction, we selected the objects from the total galaxy sample satisfying the following criteria (also see Vanzella et al. 2004). The obtained galaxy sample consists of galaxies with r-band Petrosian magnitude brighter than 17.77; the spectroscopic redshift confidence must be greater than 0.95 and there must be no warning flags. According to the restriction, we obtained the sample containing 375,929 galaxies from 582,257 data sets described in Section 4. Whereas 191,200 of the sam-

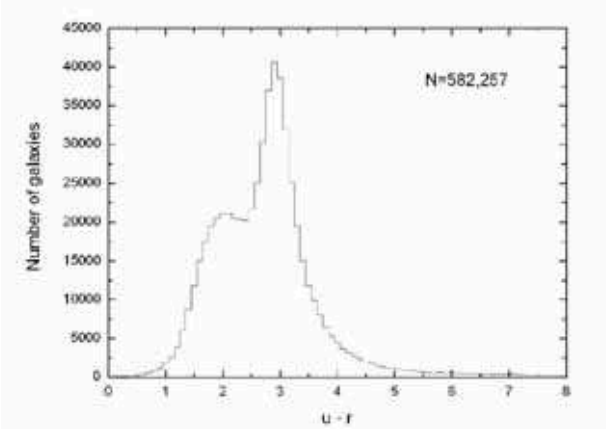

Figure 4. The $u-r$ histogram for the total galaxy samples.

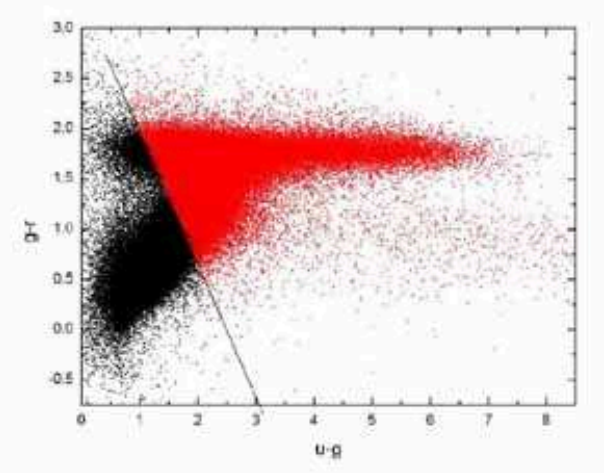

Figure 5. The $g-r$ versus $u-r$ diagram, red points represent early-type galaxies and black points represent late-type galaxies.

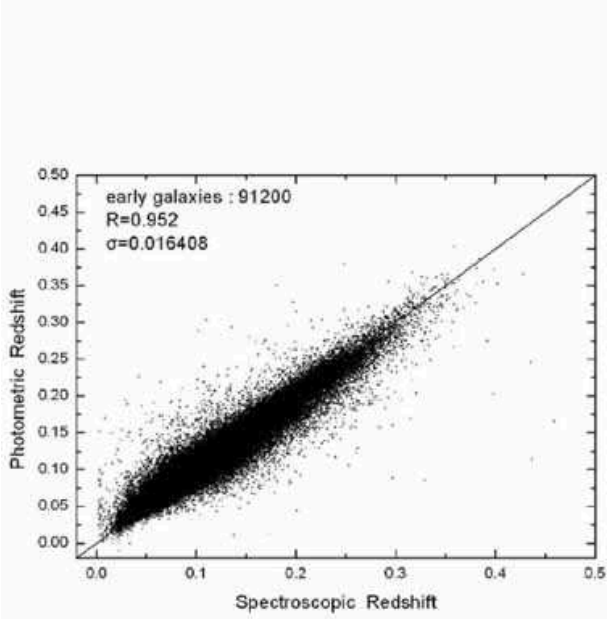

Figure 6. The comparison of predicted photometric reshifts with spectroscopic redshifts for early-type galaxies.

ple belong to early-type galaxies and 184,729 to late-type galaxies. The Galactic absorption in the different filters was obtained from the dust maps of Schlegel et al. (1998).

5.2 Result

ANNs are used to predict photometric redshifts for the selected galaxy samples. From the total sample, we randomly selected 150,000 for training, 50,000 for validation and the rest 175,929 as test sample. By training, the regressor is obtained, then it can be used to predict photometric redshifts of the test sample. The root-mean-square (rms) redshift error is represented as σ_z.

Similarly, for the early-type galaxy sample, we randomly partitioned them into 80,000 for training, 20,000 for validation and 91,200 for testing, respectively. The late-type galaxy sample was also separated into training, validation and test sets with respective sizes 80,000, 20,000 and 84,729. We also applied ANNs to predict the photometric redshifts of the two subclasses, respectively. Then calculating their mixed accuracy is as follows:

$$\sigma_{\rm mix} = \sqrt{{\sigma_{\rm early}}^2 + {\sigma_{\rm late}}^2} \tag{5}$$

$$\sigma_{\rm early} = \sqrt{\frac{1}{N_1}(\sum_{i=1}^{N_1}(zNN_i - zspec_i)^2)} \tag{6}$$

$$\sigma_{\rm late} = \sqrt{\frac{1}{N_2}(\sum_{i=1}^{N_2}(zNN_i - zspec_i)^2)} \tag{7}$$

where zNN_i is the neural output, $zspec_i$ is the target, N_1 is the test sample number of early-type galaxies, and N_2 is the test sample number of late-type galaxies. Finally, we compared the mixed accuracy with that of the total galaxy sample alone.

The experimental results with different input parameters and different samples by means of different ANN structures are given in Table 1. For different samples, the applied ANN structures are different. When applying ANNs on the actual photometric target sample, the whole procedure should be run several times with the test set by modifying the parameters of training (e.g., weight decay, the number of hidden layers) in order to optimize the performance. As shown in Table 1., it is evident that the results based on model magnitudes are better than those based on Petrosian magnitudes, while those based on dereddened magnitudes are superior to those based on model magnitudes. We also find that the performance improves when adding the parameters ($PetR50$, $PetR90$). For various situations, the rms scatter of photometric redshifts for early-type galaxies shows better performance than that for late-type galaxies. Comparing with the rms scatter of the total galaxy sample, the mixed scatter of photometric redshift estimation improves when dividing galaxies into early-type ones and late-type ones. This conclusion is similar to that of Wang et al. (2007). Especially for early-type galaxies, the result is rather better than that of late-type galaxies. For example, when taking dereddened $u, g, r, i, z, PetR50, PetR90$ as input pattern, the rms deviation of photometric redshifts for early-type galaxies adds up to 0.0164, that for late-type galaxies is 0.0217, that for the mixed sample amounts to 0.0192, and that for the total sample is 0.0196. In order to see the results clearly, the comparisons of predicted photometric reshifts with spectroscopic redshifts for early-type galaxies, late-type galaxies and the overall galaxies are plotted in Figs 6-8. These figures indicate that the experimental results for early-type and the overall galaxies show very well performance, although the result of late-type galaxies is not good. The correlation coefficient R further proves the conclusion, R is 0.0952 for early-type galaxies, 0.0881 for late-type galaxies and 0.934 for the overall galaxies. That early-type galaxies have more better accuracy of photometric redshifts than late-type ones may be due to the fact that the spectra of early-type galaxies show a more prominent break at 4000$\AA$ and therefore a better photo-z signal.

Table 1. Photometric redshift prediction with artificial neural networks

Parameters	Galaxy type	ANN structure	for Individual Subset $\sigma_{\rm early}$ or $\sigma_{\rm late}$	for Mixed Sample $\sigma_{\rm mix}$	for Total Sample $\sigma_{\rm z}$
Petrosian u, g, r, i, z	early-type	5:10:1	0.0221	0.0254	0.0264
	late-type	5:5:5:1	0.0286		
Petrosian u, g, r, i, z, PetR50, PetR90	early-type	7:5:10:1	0.0208	0.024	0.0247
	late-type	7:5:10:1	0.0271		
Model u, g, r, i, z	early-type	5:10:1	0.0178	0.0204	0.0214
	late-type	5:10:1	0.0230		
Model u, g, r, i, z, PetR50, PetR90	early-type	7:5:10:1	0.0166	0.0192	0.0203
	late-type	7:5:10:1	0.0217		
Dereddened u, g, r, i, z	early-type	5:10:1	0.0174	0.0203	0.0211
	late-type	5:10:1	0.0230		
Dereddened u, g, r, i, z, PetR50, PetR90	early-type	7:5:10:1	0.0164	0.0192	0.0196
	late-type	7:5:10:1	0.0217		

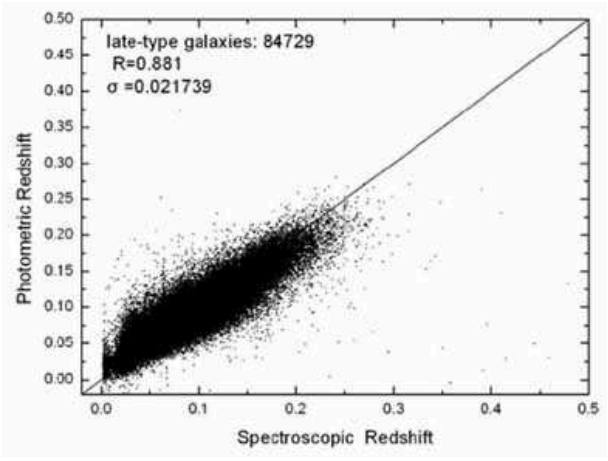

Figure 7. The comparison of predicted photometric reshifts with spectroscopic redshifts for late-type galaxies.

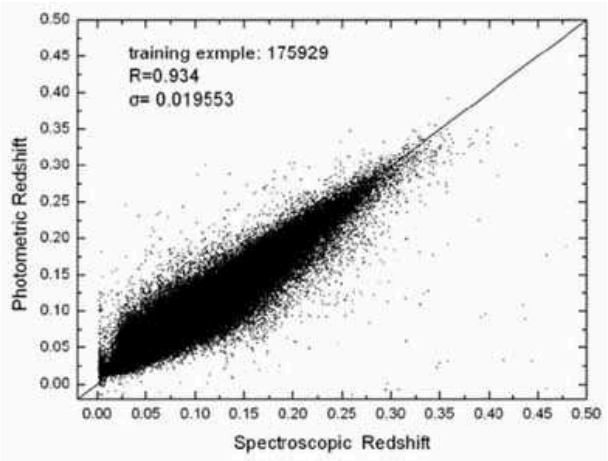

Figure 8. The comparison of predicted photometric reshifts with spectroscopic redshifts for the overall galaxies

6 CONCLUSIONS AND DISCUSSIONS

Firstly we employed an unsupervised method, k-means algorithm to subdivide the total galaxy sample into two subclasses. The objects are clustered by its intrinsic properties. By consulting the NED database, we know that the two subclasses belong to early-type galaxies and late-type galaxies, respectively. Based on the total sample and the two subsamples, we have made various experiments with different parameters for photometric redshift estimation by means of ANNs. Experimental results indicate that no matter employing Petrosian magnitudes, model magnitudes or dereddened magnitudes, the more parameters are considered, the higher the accuracy is. When the parameters are added in the training data, there will be more information for the network to improve its capability of prediction and generalization, so the final accuracy also improves correspondingly. This result is consistent with the work (Li et al. 2007). This is a typical characteristics of ANNs, which can be trained directly on problems with hundreds or thousands of inputs. Whereas for kernel regression and support vector machines (SVMs), the optimal choice of input pattern is necessary (Wang et al. 2007, 2008). Table 1 shows that the accuracy of photometric redshifts with the mixed sample outperforms that with the overall sample in different situations. The best experimental result is that the prediction accuracy is $\sigma_{\rm z} = 0.0196$ for the overall sample, $\sigma_{\rm mix} = 0.0192$ for the mixed sample,

$\sigma_{\rm early}$ = 0.0164 for early-type galaxies, $\sigma_{\rm late}$ = 0.0217 for late-type galaxies.

Up to now, there are many efforts on photometric redshifts with ANNs. Because different work is based on different samples, different attributes and different architectures, we only give a rough comparison of ANNs which are applied for photometric redshift estimation in different references, as shown in Table 2. Comparing with the former work (see Table 2), the scheme that we estimate photometric redshifts after classifying galaxies into early-type ones and late-type ones is applicable and satisfactory, moreover the scheme helps to study galaxies in detail and improve the efficiency of photometric redshift estimation. The improvement in accuracy of photometric redshift estimation is of great importance to the study of large-scale structure of the universe as well as the formation and evolution of galaxies. When the quality and quantity of observational data increases, more and more parameters are available to this problem. Moreover, ANNs will show its superiority in tackling this complex situation and have wide application (i.e. classification, regression, feature selection) in astronomy. In addition, unsupervised approaches don't require human to have the foreknowledge of the classes, and mainly using some clustering algorithm to classify data. These procedures can be used to determine the number and location of the unimodal classes and helpful for astronomers to find unusual or unknown objects or phenomenon.

7 ACKNOWLEDGMENTS

We are very grateful to referee's constructive and insightful suggestions as well as helping us improve writing. This paper is funded by National Natural Science Foundation of China under Grant Nos. 10473013, 90412016 and 10778724, and by Chinese National 863 project No.2006AA01A120. This research has made use of data products from the SDSS survey and from the Two Micron All Sky Survey (2MASS). The SDSS is managed by the Astrophysical Research Consortium for the Participating Institutions. The Participating Institutions are the American Museum of Natural History, Astrophysical Institute Potsdam, University of Basel, University of Cambridge, Case Western Reserve University, University of Chicago, Drexel University, Fermilab, the Institute for Advanced Study, the Japan Participation Group, Johns Hopkins University, the Joint Institute for Nuclear Astrophysics, the Kavli Institute for Particle Astrophysics and Cosmology, the Korean Scientist Group, the Chinese Academy of Sciences (LAMOST), Los Alamos National Laboratory, the Max-Planck-Institute for Astronomy (MPIA), the Max-Planck-Institute for Astrophysics (MPA), New Mexico State University, Ohio State University, University of Pittsburgh, University of Portsmouth, Princeton University, the United States Naval Observatory, and the University of Washington. 2MASS is a joint project of the University of Massachusetts and the Infrared Processing and Analysis Center/California Institute of Technology, funded by the National Aeronautics and Space Administration and the National Science Foundation. This research has made use of the NASA/IPAC Extragalactic Database (NED) which is operated by the Jet Propulsion Laboratory, California Institute of Technology, under contract with the National Aeronautics and Space Administration. This research has also made use of the SIMBAD database, operated at CDS, Strasbourg, France.

REFERENCES

Bailer-Jones C.A.L., Gupta R., Singh H.P., 2001, Automated Data Analysis in Astronomy, R. Gupta, H.P. Singh, C.A.L. Bailer-Jones (eds.), Narosa Publishing House, New Delhi, India, 51-68
Bailer-Jones C.A.L., 1996, PhD thesis, Univ. Cambridge
Bailer-Jones C.A.L., 2000, A&A, 357, 197
Ball N. M., Brunner R. J., Myers A. D., Strand N. E., Alberts S. L., Tcheng D., Lioráx., 2007, ApJ, 663, 774
Ball N. M., Loveday J., Fukugita M., et al. 2004, MNRAS, 3, 348
Baum W. A., 1962, in George C. M., ed, Proc. IAU Symp. 15, Photoelectric Magnitudes and Red-Shifts. Macmillan Press, New York, NY, p. 390
Bertin E., Arnouts S., 1996, A&AS, 117, 393
Bishop C. M., 1995, Neural Networks for Pattern Recognition, Oxford: Oxford University Press
Brunner R. J., Connolly A. J., Szalay A. S., Bershady M. A., 1997, ApJ, 482, L21
Bruzual A. G., Charlot S., 1993, ApJ, 405, 538
Budavári T. et al., 2005, ApJ, 619, L31
Coleman G. D., Wu C. C., Weedman D. W., 1980, ApJS, 43, 393
Collister A. A., Lahav O., 2004, PASP, 116, 345
Connolly A. J., Csabai I., Szalay A. S., Koo D. C., Kron R. G., Munn J. A., 1995, AJ, 110, 2655
Couch W. J., Ellis R. S., Godwin J., Carter D., 1983, MNRAS, 205, 1287
Csabai I. et al., 2003, ApJ, 125, 580
Curtis H.D. 1918, Pub. Lick Obs. 13, 55
D'Abrusco R., Staiano A., Longo G., Brescia M., Paolillo M., De Filippis E., Tagliaferri R., 2007, ApJ, 663, 752
Firth A. E., Lahav, O., Somerville, R. S. 2003, MNRAS, 4, 339
Firth A. E., Lahav O., Somerville R. S., 2003, MNRAS, 339, 1195
Folkes S. R., Lahav O., Maddox S. J., 1996, MNRAS, 283, 651
Gao D., Zhang Y., Zhao Y., 2008, in Robert W. Argyle, Peter S. Bunclark, and James R. Lewis., eds, ASP Conference Series, Vol.394, Astronomical Data Analysis Software and Systems, Kensington Town Hall, London, United Kingdom, p.525
Haykin S., Neural Networks: A Comprehensive Foundation, Macmillan College Publishing Company, New York, 1994
Hsieh B. C., Yee H. K. C., Lin H., Gladders M. D., 2005, ApJS, 158, 161
Hubble E. Humason M.L. 1931, ApJ, 74, 43
Levenberg K., 1944, Quarterly Journal of Applied MathematicII, 2, 164
Koo D. C., 1985, AJ, 90, 418
Lahav O., Naim A., Sodré L. J., Storrie-Lombardi M. C., 1996, MNRAS, 283, 207
Li L., Zhang Y., Zhao Y., Yang D., 2006, Progress in Astronomy, 24(4), 285
Li L., Zhang Y., Zhao Y., Yang D., 2007, ChJAA, 7, 448

[h!!!]

Table 2. The comparison of different work for predicting photometric redshifts using ANNs

References	Method	Sample	σ
Firth et al. (2003)	ANNs	EDR	0.0230
Collister & Lahav (2004)	ANNz	EDR	0.0229
Vanzella et al. (2004)	MLP	DR1	0.0220
Li et al. (2007)	MLP	DR2	0.0202
D'Abrusco et al. (2007)	MLP	DR5	0.0208
this work	ANNs	DR5	0.0192

MacQueen J. B., 1967, Proceedings of 5-th Berkeley Symposium on Mathematical Statistics and Probability, Berkeley, University of California Press, 1:281-297
Marquardt D. W., 1963, Journal of the Society of Industrial and Applied Mathematics, 11, 431
Melnick J., Sargent W.L.W. 1977, ApJ, 215, 401
Miller, A. S.1993, Vistas in Astronomy36(2), 141
Nadaraya E. A., 1964, Theory of Probability and its Applications, 9, 141
Nielsen M. L., Odewahn S. C., 185th AAS Meeting, 1994, 26, 1498
Odewahn S. C., Nielsen M.L., 1994, Vistas in Astronomy, 3, 38
Oemler A. Jr. 1974, ApJ 194, 1
Serra-Ricart M., Calbet X., Garrido L., Gaitan V., 1993, AJ, 106, 1685
Schlegel D. J., Finkbeiner D. P., Davis M., 1998, ApJ, 500, 525
Shimasaku, K., et al. 2001, AJ, 122, 1238
Storrie-Lombardi M. C., Lahav O., 1994, guest eds, Vistas in Astron., spec. iss. on ANNs in Astronomy, 38 (3)
Strateva I. et al., 2001, AJ, 122, 1861
Suchkov A. A., Hanisch R. J., Margon B., 2005, AJ, 130, 2439
Vanzella E. et al., 2004, A&A, 423, 761
Wadadekar Y., 2005, PASP, 117, 79
Wang D., Zhang Y., Liu C., Zhao Y., 2007, MNRAS, 382, 1601
Wang D., Zhang Y., Liu C., Zhao Y., 2008, ChJAA, 8(1), 119
Wang Y., Bahcall N., Turner E. L., 1998, AJ, 116, 2081
Way M. J., Srivastava A. N., 2006, ApJ, 647, 102
Weaver W. B., 2000, ApJ, 1, 541
York D. G. et al., 2000, AJ, 120, 1579
Zhang Y., Zhao Y., 2004, A&A, 422, 1113
Zhang Y., Zhao Y., 2007, ChJAA, 7, 289